International Journal of u- and e- Service, Science and Technology
Vol.8, No. 7 (2015), pp.379-386
http://dx.doi.org/10.14257/ijunesst.2015.8.7.38

Performance Analysis of the M2M Network over Keyhole Nakagami Fading Channels

Lingwei Xu[1], Hao Zhang[1,2], Tingting Lu[1], Zengfeng Wang[1] and T. Aaron Gulliver[2]

[1]*College of Information Science and Engineering, Ocean University of China, Qingdao 266100, China*
[2]*Department of Electrical and Computer Engineering, University of Victoria, Victoria, BC V8W 2Y2, Canada*
gaomilaojia2009@163.com, zhanghao@ouc.edu.cn, lvtingting33@163.com, agullive@ece.uvic.ca

Abstract

The performance of the mobile-to-mobile (M2M) network over keyhole Nakagami fading channels is investigated in this paper. Using the method of the probability density function (PDF) of the signal-to-noise ratio (SNR), the exact and approximate closed-form average symbol error probability (ASEP) expressions are derived for pulse-amplitude modulation (PAM), phase shift keying (PSK),and frequency shift keying modulation (FSK). The exact closed-form expressions for channel capacity are also presented. Then the ASEP and channel capacity performance under different conditions is evaluated through numerical simulations to verify the analysis. The simulation results showed that the performance of the M2M network is improved with the transmitting/receiving antennas and the fading coefficient increased.

Keywords: *M2M communication, orthogonal space-time block code, keyhole Nakagami fading channels, average symbol error probability, channel capacity*

1. Introduction

In recent years, mobile-to-mobile (M2M) communication is widely employed in many popular wireless communication systems, such as mobile ad-hoc networks and vehicle-to-vehicle networks [1]. Multiple-input-multiple-output (MIMO) technology has emerged as a promising solution for M2M communication [2]. The use of multiple transmit and receive antennas can potentially provide a large improvement in spectral efficiency and reliability for wireless communication in the presence of multipath fading[3-5].To this end, several transmit diversity techniques have been proposed, such as space-time trellis code (STTC) [6], and space-time block code (STBC) [7]. STBC can effectively achieve the transmit diversity by the use of MIMO technology, especially the orthogonal STBC with low decoding complexity can obtain full diversity gain which can greatly improve the reliability of mobile communication system.

In realistic propagation environments, both theoretical analysis and experimental results indicate that keyhole fading is a more suitable channel model [8-10]. In [11], by the moment generating function (MGF) method, the authors analyzed the performance of orthogonal STBC in keyhole MIMO channels. Closed-form expressions for the error probability of orthogonal STBC as well as diversity gains of keyhole channels were derived. Using the MGF method, [12] extended the work in [11] to more general cases where coherent phase-shift keying (PSK) and quadrature amplitude modulation (QAM) schemes were employed. The exact symbol error rate (SER) expressions for a relay system with orthogonal STBC over correlated/keyhole fading channels were derived in

ISSN: 2005-4246 IJUNESST

[13]. It also analyzed the outage probability of interference corrupted relay systems with maximal ratio combing (MRC) at the receiver.

However, to the best knowledge of the author, most of the results for keyhole fading have been obtained using the MGF method. Thus, the probability density function (PDF) of the SNR has not been considered. Motivated by all of the above, in this paper, the PDF of the SNR is employed to derive the exact and approximate closed-form expressions for the average symbol error probability (ASEP) and channel capacity of the M2M system over keyhole Nakagami fading channels. The main contributions are listed as follows:

First, we provide closed-form expressions for probability density function (PDF) of the signal-to-noise ratio (SNR) after STBC decoding. Then, we use those PDF expressions to derive closed-form ASEP expressions for PAM, PSK, and FSK modulations. The exact closed-form expressions for channel capacity are also presented. In order to show the accuracy of the analytical results, the ASEP and channel capacity performance under different conditions is evaluated through numerical simulations. Results are presented which show that the fading coefficients and the transmitting/receiving antennas have a significant influence on the ASEP and channel capacity performance.

The rest of the paper is organized as follows. Section 2 presents the system model. In Section 3, the closed-form ASEP expressions are derived for different modulation schemes. Section 4 presents the exact closed-form expressions for channel capacity. Section 5 presents some numerical results to illustrate and verify the analysis given in the previous section, and Section 6 provides some conclusions.

2. The System Model

We consider a MIMO network with K transmitting antennas and M receiving antennas. The channel is assumed to be quasi-static with flat fading, which means that the channel is constant within one frame period, but varies independently between frames. Furthermore, perfect channel state information is assumed available at the receiver, but the channel is unknown at the transmitter.

The input information sequences are respectively encoded using FSK/PAM/PSK modulation, and output S symbols. Then through space-time block codes, S symbols are transmitted from K transmit antennas. At the receiver, the received signal is given by

$$Y = HX + W \tag{1}$$

where Y is the complex received signal matrix , X is the complex transmitted signal matrix, and W is the additive noise matrix with independent and identical distributed entries of $CN(0,N_0/2)$, N_0 is the power spectral density of the additive noise.

In a wireless MIMO channel with keyhole effects, all the signals transmitted from K transmitters to M receivers have to pass through a keyhole. As a result, the channel matrix subject to keyhole effects can be written as [11]

$$H = gab = g\begin{bmatrix} a_1b_1 & a_2b_1 & \cdots & a_Kb_1 \\ a_1b_2 & a_2b_2 & \cdots & a_Kb_2 \\ \vdots & \vdots & \vdots & \vdots \\ a_1b_M & a_2b_M & \cdots & a_Kb_M \end{bmatrix} \tag{2}$$

where g denotes the propagation loss, the column vectors $\boldsymbol{a}=[a_1, a_2, \ldots, a_K]^T$, and $\boldsymbol{b}=[b_1, b_2, \ldots, b_M]$ describe the rich scattering at the transmitting and receiving antennas, respectively. a_i and b_j follow the Nakagami distribution , the density functions can be given as

$$f_{a_i}(a) = \frac{2m_t^{m_t}}{\Omega_t^{m_t}\Gamma(m_t)} a^{2m_t-1}\exp(-\frac{m_t}{\Omega_t}a^2) \tag{3}$$

$$f_{b_j}(b) = \frac{2 m_r^{m_r}}{\Omega_r^{m_r} \Gamma(m_r)} b^{2m_r - 1} \exp(-\frac{m_r}{\Omega_r} b^2) \tag{4}$$

where m_t and m_r are fading coefficients, Ω_t and Ω_r are scaling factors.

In [14], when an orthogonal STBC is used, the authors proposed a scalar additive white Gaussian noise (AWGN) channel approach, which can transform a MIMO fading channel into an AWGN channel. Based on the AWGN channel approach, the signal after STBC decoding is defined as

$$y = \|H\|_F^2 x + w \tag{5}$$

where $\|H\|_F^2$ is the squared Frobenius norm of H.

Taking into account the code rate R, the scaled AWGN channels with an orthogonal STBC is given by

$$y = \frac{1}{R}\|H\|_F^2 x + w \tag{6}$$

where y is the $S\times 1$ complex matrix after STBC decoding from the received matrix Y, x is $S\times 1$ complex matrix after FSK/PAM/PSK modulation, and w is the $S\times 1$ additive noise matrix with independent and identical distributed entries of $CN(0,1/\mathrm{R}\times\|H\|_F^2\times N_0/2)$.

Here, we assume that the propagation loss g=1.Therefore, the effective instantaneous SNR, denoted as r_s, at the receiver is

$$r_s = \frac{E_s}{KRN_0}\|H\|_F^2 = \frac{E_s}{KRN_0}\|a\|^2\|b\|^2 = \frac{E_s}{KRN_0}\sum_{i=1}^{K}\sum_{j=1}^{M} a_i^2 b_j^2 \tag{7}$$

where E_s is the total transmitted power.

We define that

$$Q = \|a\|^2\|b\|^2 = \sum_{i=1}^{K}\sum_{j=1}^{M} a_i^2 b_j^2 \tag{8}$$

The PDF of Q is given as [15]

$$f_Q(p) = \frac{2(\frac{\Omega_t\Omega_r}{m_t m_r})^{-(Km_t+Mm_r)/2}}{\Gamma(Km_t)\Gamma(Mm_r)} p^{(Km_t+Mm_r)/2-1} K_{Km_t-Mm_r}(2\sqrt{\frac{m_t m_r}{\Omega_t\Omega_r}p}) \tag{9}$$

where $\Gamma(\cdot)$ is the Gamma function, $K_v(\cdot)$is the vth modified Bessel function of the second kind [16].

So the PDF of r_s is given as [15]

$$p(r_s) = \frac{2R(\frac{\Omega_t\Omega_r}{m_t m_r})^{-(Km_t+Mm_r)/2}}{r_p\Gamma(Km_t)\Gamma(Mm_r)}(\frac{r_s}{r_p}R)^{(Km_t+Mm_r)/2-1} K_{Km_t-Mm_r}(2\sqrt{\frac{m_t m_r}{\Omega_t\Omega_r}R\frac{r_s}{r_p}}) \tag{10}$$

where

$$r_p = \frac{E_s}{KN_0} \tag{11}$$

For the simplicity, we define that

$$\alpha = Km_t - Mm_r, \beta = \frac{m_t m_r}{\Omega_t\Omega_r}\times\frac{R}{r_p}, \gamma = \frac{Km_t+Mm_r}{2} \tag{12}$$

So (10) can be rewritten as

$$p(r_s) = \frac{2(\beta)^{\gamma}}{\Gamma(Km_t)\Gamma(Mm_r)}(r_s)^{\gamma-1} K_{\alpha}(2\sqrt{\beta r_s}) \tag{13}$$

3. Average Symbol Error Probability

The ASEP averaged over the fading SNR is given by [17]

$$P = \int_0^{\infty} P_q(r_s)\, p(r_s)\, dr_s \tag{14}$$

where $P_q(x)$ denotes the SEP of the q-ary modulation employed.

3.1. FSK

The SEP of q-ary FSK modulation in an AWGN channel is given by[17]

$$P_q(r_s) = \sum_{n=1}^{q-1} \frac{(-1)^{n+1}}{n+1} \binom{q-1}{n} e^{-r_s \frac{n}{n+1}} \tag{15}$$

Substituting (13) and (15) into (14), the ASEP of q-ary FSK is given as

$$P_{FSK}(r_s) = \frac{2(\beta)^{\gamma}}{\Gamma(Km_t)\Gamma(Mm_r)} \times \sum_{n=1}^{q-1} \frac{(-1)^{n+1}}{n+1} \binom{q-1}{n} \times V \tag{16}$$

$$V = \int_0^{\infty} e^{-r_s \frac{n}{n+1}} (r_s)^{\gamma-1} K_{\alpha}(2\sqrt{\beta r_s})\, dr_s \tag{17}$$

To evaluate the integral in (17), the following integral function can be employed [16]

$$\begin{aligned} &\int_0^{\infty} e^{-ax} (x)^{\mu-\frac{1}{2}} K_{2\nu}(2\delta\sqrt{x})\, dx \\ &= \frac{\Gamma(a+\nu+\frac{1}{2})\Gamma(a-\nu+\frac{1}{2})}{2\delta} \exp\left(\frac{\delta^2}{2a}\right) a^{-\mu} W_{-\mu,\nu}\left(\frac{\delta^2}{a}\right) \\ &\left[\mathrm{Re}\left(\mu+\nu+\frac{1}{2}\right)\right] > 0 \end{aligned} \tag{18}$$

where $W_{\lambda,\mu}(\cdot)$ is the Whittaker function[16].

So (17) can be given as

$$V = \frac{\Gamma\left(\frac{n}{n+1}+\frac{\alpha}{2}+\frac{1}{2}\right)\Gamma\left(\frac{n}{n+1}-\frac{\alpha}{2}+\frac{1}{2}\right)}{2\sqrt{\beta}} \exp\left(\frac{\beta(n+1)}{2n}\right) \left[\frac{n+1}{n}\right]^{\gamma-0.5} W_{-\gamma+0.5,\alpha/2}\left(\frac{\beta(n+1)}{n}\right) \tag{19}$$

3.2. PAM

The SEP of q-ary PAM in an AWGN channel is given by[17]

$$P_q(r_s) = 2\left(1-\frac{1}{q}\right) Q\left(\sqrt{\frac{6r_s}{q^2-1}}\right) \tag{20}$$

where $Q()$ is the Gaussian tail function.

Substituting (13) and (20) into (14), the ASEP of q-ary PAM is given as

$$P_{PAM}(r_s) = \frac{4(\beta)^{\gamma}}{\Gamma(Km_t)\Gamma(Mm_r)} \times \left(1-\frac{1}{q}\right) \times V_1 \tag{21}$$

$$\begin{aligned} V_1 &= \int_0^{\infty} Q\left(\sqrt{\frac{6r_s}{q^2-1}}\right)(r_s)^{\gamma-1} K_{\alpha}(2\sqrt{\beta r_s})\, dr_s \\ &= \frac{1}{2}\int_0^{\infty} erfc\left(\sqrt{\frac{3r_s}{q^2-1}}\right)(r_s)^{\gamma-1} K_{\alpha}(2\sqrt{\beta r_s})\, dr_s \end{aligned} \tag{22}$$

To evaluate the integral in (22), the following integral function can be employed [18]

$$erfc(\sqrt{Br}) = \frac{1}{\sqrt{\pi}} G_{1,2}^{2,0}\left[Br \middle|_{0,0.5}^{1} \right] \tag{23}$$

$$G_{0,2}^{2,0}\left[z \middle|_{b,c}^{-} \right] = 2z^{\frac{1}{2}(b+c)} K_{b-c}(2\sqrt{z}) \tag{24}$$

where G[·] is the Meijer's G-function [16].

So we can obtain

$$\begin{aligned} V_1 &= \int_0^{\infty} \frac{1}{4\sqrt{\pi}} G_{1,2}^{2,0}\left[\frac{3r_s}{q^2-1} \middle|_{0,0.5}^{1} \right] (r_s)^{\gamma-1} G_{0,2}^{2,0}\left[\beta r_s \middle|_{\alpha/2,-\alpha/2}^{-} \right] dr_s \\ &= \frac{1}{4\sqrt{\pi}} \int_0^{\infty} (r_s)^{\gamma-1} G_{0,2}^{2,0}\left[\beta r_s \middle|_{\alpha/2,-\alpha/2}^{-} \right] G_{1,2}^{2,0}\left[\frac{3r_s}{q^2-1} \middle|_{0,0.5}^{1} \right] dr_s \\ &= \frac{\beta^{-\gamma}}{4\sqrt{\pi}} G_{3,2}^{2,2}\left[\frac{3}{\beta(q^2-1)} \middle|_{0,0.5}^{1-\gamma-\alpha/2,1-\gamma+\alpha/2,1} \right] \end{aligned} \tag{25}$$

3.3. PSK

The SEP of *q*-ary PSK modulation in an AWGN channel is given by [17]

$$P_q(r_s) = 2Q\left(\sqrt{2\sin^2\frac{\pi}{q} r_s}\right) - \frac{1}{\pi} \int_{\frac{\pi}{2}-\frac{\pi}{q}}^{\frac{\pi}{2}} e^{-r_s \frac{\sin^2 \pi/q}{\cos^2\theta}} d\theta \tag{26}$$

For large SNR and large values of *q*, the SEP of *q*-ary PSK in an AWGN channel can be approximated as

$$P_q(r_s) \approx 2Q\left(\sqrt{2\sin^2\frac{\pi}{q} r_s}\right) \tag{27}$$

Substituting (27) into (14), the ASEP of *q*-ary PSK can be approximated as

$$P_{PSK}(r_s) \approx \frac{4(\beta)^{\gamma}}{\Gamma(Km_t)\Gamma(Mm_r)} V_2 \tag{28}$$

where

$$\begin{aligned} V_2 &= \int_0^{\infty} Q\left(\sqrt{2\sin^2\frac{\pi}{q} r_s}\right) (r_s)^{\gamma-1} K_{\alpha}(2\sqrt{\beta r_s}) dr_s \\ &= \frac{1}{2} \int_0^{\infty} erfc\left(\sqrt{\sin^2\frac{\pi}{q} r_s}\right) (r_s)^{\gamma-1} K_{\alpha}(2\sqrt{\beta r_s}) dr_s \\ &= \frac{1}{4\sqrt{\pi}} \int_0^{\infty} (r_s)^{\gamma-1} G_{0,2}^{2,0}\left[\beta r_s \middle|_{\alpha/2,-\alpha/2}^{-} \right] G_{1,2}^{2,0}\left[\sin^2\frac{\pi}{q} r_s \middle|_{0,0.5}^{1} \right] dr_s \\ &= \frac{\beta^{-\gamma}}{4\sqrt{\pi}} G_{3,2}^{2,2}\left[\frac{\sin^2\frac{\pi}{q}}{\beta} \middle|_{0,0.5}^{1-\gamma-\alpha/2,1-\gamma+\alpha/2,1} \right] \end{aligned} \tag{29}$$

4. Average Channel Capacity

The average capacity over an keyhole Nakagami channel is given as [17]

$$C = \int_0^{\infty} \log_2(1+r_s) p(r_s) dr_s \tag{30}$$

To facilitate the calculation, we can rewrite (30) as

$$C = \log_2(e) \int_0^{\infty} \ln(1+r_s) p(r_s) dr_s \tag{31}$$

To evaluate the integral in (31), the following integral function can be employed [16]

$$\ln(1+r) = G_{2,2}^{1,2}\left(r \middle|_{1,0}^{1,1}\right) \tag{32}$$

Substituting (32) into (31), we can obtain

$$C = \frac{(\beta)^{\gamma} \log_2(e)}{\Gamma(Km_t)\Gamma(Mm_r)} \int_0^{\infty} (r_s)^{\gamma-1} G_{2,2}^{1,2}(r_s \Big|_{1,0}^{1,1}) G_{0,2}^{2,0}\left[\beta r_s \Big|_{\alpha/2,-\alpha/2}^{-}\right] dr_s \quad (33)$$

$$= \frac{(\beta)^{\gamma} \log_2(e)}{\Gamma(Km_t)\Gamma(Mm_r)} G_{2,4}^{4,1}\left[\beta \Big|_{\alpha/2,-\alpha/2,-\gamma,-\gamma}^{-\gamma,1-\gamma}\right]$$

5. Numerical Results

In this section, we present Monte-Carlo simulations and numerical methods to confirm the derived analytical results. Additionally, random number simulation was done to confirm the validity of the analytical approach. All the computations were done in MATLAB and some of the integrals were verified through MAPLE. The links are modeled as keyhole Nakagami distribution. For the simplicity, we use the (*K*, *M*, *m*; *K*×*M*×*m*) to represent the antenna configuration and fading coefficient of the M2M network.

Figure1 presents the impact of the number of transmitting/receiving antennas on the ASEP of the M2M network over keyhole Nakagami fading channels with BPAM. The number of transmitting antennas is *K*=2,3, the number of receiving antennas is *M*=2,4, the fading coefficients are m_t=m_r=2. Simulation results show that the ASEP performance is improved with the number of transmitting/receiving antennas increased. For example, when SNR=6dB, the ASEP of (2,2,2;8) is 6.1×10^{-3},(3,2,2;12) is 4.4×10^{-3}, (2,4,2;16) is 5.8×10^{-4}. With the increase of SNR, the ASEP is reduced gradually.

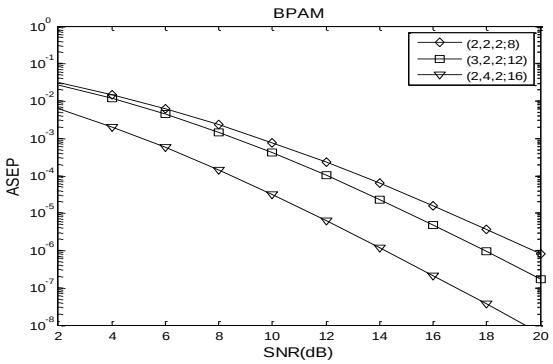

Figure 1. The Impact of the Number of Transmitting/Receiving Antennas on the ASEP of the M2M Network with BPAM

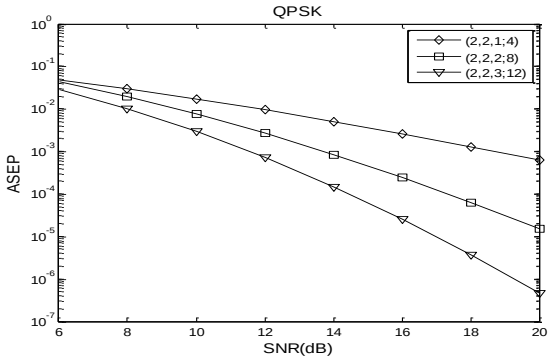

Figure 2. The Impact of the Fading Coefficient on the ASEP of the M2M Network with QPSK

Figure 2 presents the impact of the fading coefficient on the ASEP of the M2M

network with QPSK. The number of transmitting antennas is K=2, the number of receiving antennas is M=2, the fading coefficients are m_t=m_r=1,2,3. Simulation results show that the fading coefficients have a significant impact on the ASEP performance. With the increase of the fading coefficients, the ASEP is reduced gradually. For example, when SNR=10dB, the ASEP of (2,2,1;4) is 1.7×10^{-2},(2,2,2;8) is 7×10^{-3}, (2,2,3;12) is 3×10^{-3}. With the increase of SNR, the ASEP over keyhole Nakagami fading channels is reduced gradually.

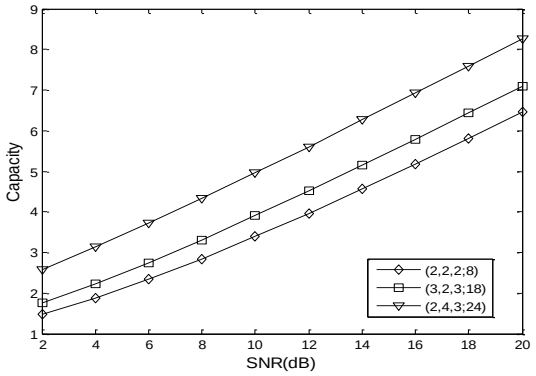

Figure 3. The Capacity of the M2M Network

Figure 3 presents the capacity of the M2M network over keyhole Nakagami fading channels. The number of transmitting antennas is K=2,3, the number of receiving antennas is M=2,4; the fading coefficients are m_t=m_r=2,3. Simulation results show that the capacity performance can be improved with the increase of transmitting/receiving antennas, and the fading coefficient. For example, when SNR=10dB, the capacity of (2,2,2;8) is 3.4bps/Hz,(3,2,3;18) is 3.9bps/Hz, (2,4,3;24) is 5bps/Hz. With the increase of SNR, the capacity over keyhole Nakagami fading channels is increased gradually.

6. Conclusions

The ASEP and channel capacity performance of the M2M network over keyhole Nakagami fading channels is investigated in this paper. The exact and approximate closed-form ASEP and channel capacity expressions are presented. The simulation results showed that the performance of the M2M network is improved with the transmitting/receiving antennas and the fading coefficient increased. The derived ASEP and channel capacity expressions can be used to evaluate the performance of the vehicular communication systems such as inter-vehicular communications, intelligent highway applications and mobile ad-hoc applications. In the future, we will consider the impact of the correlated channels on the performance of the M2M network.

Acknowledgments

The authors would like to thank the referees and editors for providing very helpful comments and suggestions. This project was supported by National Natural Science Foundation of China (no. 61304222, no. 61301139), Natural Science Foundation of Shandong Province (no.ZR2012FQ021), the Shandong Province Outstanding Young Scientist Award Fund (no. 2014BSE28032), International Science&Technology Cooperation Program of Qingdao (no.12-1-4-137-hz).

References

[1] S. Mumtaz, K. M. S. Huq and J. Rodriguez, "Direct mobile-to-mobile communication: Paradigm for 5G," IEEE Wireless Communications, vol. 21, no. 5, **(2014)**, pp. 14-23.
[2] L. Yan, S. Feng, Y. J. Zhang, B. Stevan. "Joint IQ Imbalance and Channel Estimation for MIMO-OFDM Systems with Sparse Multipath Channels," Journal of Electronics & Information Technology, vol. 35, no. 2, **(2013)**, pp. 280-284.
[3] Z. X. Fang, X. J. Yuan, and X. Wang. "Towards the Asymptotic Sum Capacity of the MIMO Cellular Two-Way Relay Channel," IEEE Transactions on Signal Processing, vol. 62, no. 6, **(2014)**, pp. 4039-4051.
[4] X. Yuan, T. Yang, I. B. Collings. "Multiple-input multiple-output two-way relaying: A space-division approach," IEEE Transactions on Information Theory, vol. 59, no. 5, **(2013)**, pp. 6421-6440.
[5] D. A. Basnayaka, P. J. Smith, P. A. Martin. "Performance Analysis of Macrodiversity MIMO Systems with MMSE and ZF Receivers in Flat Rayleigh Fading," IEEE Transactions on Wireless Communications, vol. 12, no. 5, **(2013)**, pp. 2240-2251.
[6] K. R. Kumar, G. Caire. "Space-Time Codes from Structured Lattices," IEEE Transactions on Information Theory, vol. 55, no. 2, **(2009)**, pp. 547-556.
[7] R. Vehkalahti, C. Hollanti, and F. Oggier. "Fast-Decodable Asymmetric Space-Time Codes From Division Algebras," IEEE Transactions on Information Theory, vol. 58, no.4, **(2012)**, pp. 2362-2385.
[8] S. Sanayei, A. Nosratinia. "Antenna Selection in Keyhole Channels," IEEE Transactions on Communications, vol. 55, no. 3, **(2007)**, pp. 404-408.
[9] C. Zhong, T. Ratnarajah, K. K. Wong, M. S. Alouini. "Effective capacity of multiple antenna channels: correlation and keyhole," IET Communications, vol. 6, no.12, **(2012)**, pp.1757-1768.
[10] T. Zhang. "Performance analysis of cooperative multiple- input multiple-output relaying with orthogonal space-time block codes (STBCs) in the presence of keyhole effects," IET Communications, vol. 6, no.13, **(2012)**, pp.1943-1951.
[11] Y. Gong, K. B. Letaief. "On the Error Probability of Orthogonal Space-Time Block Codes over Keyhole MIMO Channels," IEEE Transactions on Wireless Communications, vol. 6, no. 9, **(2007)**, pp. 3402-3409.
[12] H. Z. Zhao, Y. Gong, Y. L. Guan, Y. X. Tang. "Performance Analysis of M-PSK/M-QAM Modulated Orthogonal Space-ime Block Codes in Keyhole Channels," IEEE Transactions on Vehicular Technology, vol. 58, no.2, **(2009)**, pp. 1036-1043.
[13] L. Yang, M. S. Alouini, K. Qaraqe, W. P.Liu. "On the Performance of Dual-Hop Systems with Multiple Antennas: Effects of Spatial Correlation, Keyhole, and Co-Channel Interference," IEEE Transactions on Communications, vol. 60, no.12, **(2012)**, pp.3541-3547.
[14] S. Sandhu, A. Paulraj. "Space-time block codes: A capacity perspective," IEEE Communication Letters, vol.4, no.12, **(2000)**, pp.384-386.
[15] H. Shin and J. H. Lee, "Performance analysis of space-time block codes over keyhole Nakagami-m fading channels," IEEE Transactions on Vehicular Tecnology, vol. 53, **(2004)**, pp. 351-361.
[16] I. S. Gradshteyn, and I. M. Ryzhik, Table of Integrals, Series, and Products, 6th ed. San Diego: Academic Press, **(2000)**.
[17] J. G. Proakis. Digital Communications, 4th Ed, McGraw-Hill, **(2001)**.
[18] "The Wolfram functions site." [Online]. Available: http://functions.wolfram.com.

Author

Lingwei Xu was born in Gaomi, Shandong Province, China, in 1987. He received his M.Sc. degree from Ocean University of China, Qingdao, China, in 2013. He is currently working toward the Ph.D. degree. His research interests include 60GHz wireless communication, MIMO wireless communication, and channel coding theory.

